Catal Lett (2008) 120:236–243
DOI 10.1007/s10562-007-9275-6

Investigation of Pt Catalysts Supported on Multi-Walled Carbon Nanotubes with Various Diameters and Lengths

Ying Liang · Jun Li · Shi-Zhong Wang · Xian-Zhu Fu · \Qing-Chi Xu · Jing-Dong Lin · Dai-Wei Liao

Received: 16 July 2007 / Accepted: 10 September 2007 / Published online: 29 September 2007

Abstract Platinum electrocatalysts supported on multi-walled carbon nanotubes (MWCNTs) with various diameters and lengths were studied by using transmission electron microscopy (TEM), X-ray photoelectron spectroscopy (XPS), and cyclic voltammetry (CV) and Chronoamperometry. The results indicated that the MWCNTs with smaller diameter generated more amorphous carbon after a sonochemical oxidation treatment. Compared with the long MWCNTs, the short MWCNTs had more open ends, resulting in high-Pt dispersion and electrocatalytic activity towards methanol oxidation. Pt nanoparticles supported on short MWCNTs with a diameter of 30–50 nm exhibited the best Pt dispersion and highest methanol oxidation activity among the catalysts studied. The high activities of the catalysts based on short MWCNTs were due to both the intrinsic high activity of the ends of MWCNTs and a good Pt distribution.

Keywords Multi-walled carbon nanotubes · Platinum · Methanol oxidation · Diameter and length

Y. Liang · S.-Z. Wang · X.-Z. Fu · Q.-C. Xu · J.-D. Lin · D.-W. Liao (✉)
The State Key Laboratory of Physical Chemistry on Solid Surfaces, Department of Chemistry, College of Chemistry and Chemical Engineering, Institute of Physical Chemistry, Xiamen University, Xiamen 361005, China
e-mail: dwliao@xmu.edu.cn

Y. Liang
e-mail: lyingair@126.com

J. Li
College of Power Engineering, Chongqing University, Chongqing 400030, China

1 Introduction

Carbon nanotubes (CNTs) have attracted more and more interest in the applications of the new carbon materials in a variety of fields, including chemical and biological sensors [1, 2], separation membranes [3, 4], field emission devices [5, 6], energy storage [7, 8]. CNTs are widely studied as supports of depositing metal nanoparticles as heterogeneous catalysts due to their extraordinary structure, good electronic conductivity and improved accessibility of reactants to the active sites [9, 10]. For instance, Ru, Pd, Au and Pb were deposited on carbon nanobutes and resulted in good catalytic activity [11–14].

The CNTs have also attracted great attention as supports for Pt and Pt alloy catalysts in low-temperature fuel cell [15–22]. Studies have shown that the Pt base catalysts supported on CNTs may provide improved electrocatalytic activity compared to the catalysts on the traditional Vulcan XC-72 carbon support in fuel cell. The improvement catalytic activity can be usually attributed to various causes [15–18], including (a) higher electronic conductivity of CNTs, (b) higher electrochemical surface area (ECSA), (c) decreased impurities in the CNTs when compared with the Vulcan carbon, (d) higher durability during the electrochemical conditions. Huang et al. [22] showed that Pt supported on single-walled carbon nanotubes (SWCNTs) exhibited higher methanol oxidation performance than that on Vulcan XC-72 carbon due to the large number of surface functional groups and open ends of the CNTs.

Moreover, the deposition, distribution and crystallite size of Pt nanoparticles supported on CNTs are significantly affected by factors including the oxidation treatment of CNTs, the structure of CNTs and the surface area of CNTs [23–25]. Li et al. [23] have studied the

SWCNTs, double-walled carbon nanotubes (DWCNTs) and multi-walled carbon nanotubes (MWCNTs) as fuel cell catalyst supports systematically and showed the DWCNTs supported catalysts exhibited the highest activity for methanol oxidation reaction. Yuan and co-workers [24] reported that Pt supported on MWCNTs with a diameter of 15 nm had better Pt dispersion and higher electrochemical activities for methanol oxidation than that on MWCNTs with a diameter of 25 nm. However, the factors affecting Pt dispersion were not discussed in detail.

In this work, the effect of both the diameter and the length of MWNCTs on the dispersion and electrocatalytic activity of Pt nanoparticles were studied. An enhancement of the electrocatalytic activity by the ends of MWNCTs was reported.

2 Experimental

2.1 Purification and treatment of MWCNTs

Multi-walled carbon nanotubes with different diameters and lengths were purchased from Chengdu Timenano Co. Ltd., and Shenzhen Nanotech Port Co. Ltd., Chengdu, China. All the MWCNTs were synthesis by CVD method. The CNTs are abbreviated as Dxx-y in this work, where the xx stands for the tube diameter (nm), the y stands for the tube length (μm). For example, D3050-2 means that the diameter of carbon nanotube is about 30–50 nm, and the tube length is about 2 μm. The CNTs were pre-treated in a flask containing a mixture of 8 M HNO_3 and 8 M H_2SO_4 [26, 27]. The flask was placed in an ultrasonic bath (100 W, 40 kHz) at 60 °C for 3 h. The MWCNTs were then centrifuged and filtered with de-ionized water for several times and dried at 80 °C for 12 h.

2.2 Preparation of MWCNTs supported Pt catalysts

Microwave-assisted polyol process was used to prepare a series of MWCNTs supported Pt catalysts. First, 0.04 g MWCNTs was ultrasonically mixed with 25 ml ethylene glycol (EG) solution to form a homogeneous suspension. Then, 1.25 ml 0.0386 M $H_2PtCl_6 \cdot 6H_2O$ EG solution and 0.6 ml 0.4 M KOH EG solution were added drop by drop into the mixture. After stirring for 10 h, the suspensions were ultrasonically treated for 30 min and then heated in a microwave oven (Galanz 2,450 MHz, 700 W) for 60 s. Finally, the suspensions were filtrated and washed with de-ionized water, and then dried in a vacuum oven at 80 °C for 10 h. The Pt loadings in all the catalysts (abbreviated as Pt/Dxx-y) were 20 wt.%.

2.3 Physical characterization

The surface area of MWCNTs was measured by using physical adsorption of N_2 at 77 K (Micromeritic Tristar 3000). The adsorption isotherms were used to calculate the values of BET specific surface area. The conductivities of MWCNTs of fresh and after acids oxidation were measured by conventional four-point probe method. X-ray photoelectron spectroscopy (XPS) analysis was carried out with a PHI Quantum 2000 Scanning ESCA Microprobe equipment (Physical Electronics, MN, USA) using monochromatic Al-Ka radiation. The X-ray beam diameter was 100 μm, and the pass energy was 29.35 eV for all the samples. The binding energy was calibrated with respect to C (1s) at 284.6 eV. Transmission electron microscopy (TEM) measurement was performed on a Tecnai F-30 microscope and JEM-2100HC at 300 kV or 200 KV to characterize the Pt distribution and morphology of the catalysts. A drop of sample was ultrasonic treated and deposited on a cupper grid coated with a continuous carbon film.

2.4 Electrochemical measurement

The electrochemical characterization was carried out with a CHI660A electrochemical workstation. Glassy carbon (GC) electrode coated with catalyst ink was used as the working electrode. Pt foil and saturated calomel electrode (SCE) were used as a counter electrode and reference electrode, respectively. The working electrode was prepared as follows. The GC (4 mm diameter) electrode was polished carefully by using 0.3 and 0.05 μm alumina pastes. A MWCNTs paste with a concentration of 1 mg ml^{-1} was prepared by mixing suitable amount of MWCNTs with 0.1% Nafion solution. Then 15 μl of the electrode paste was placed on top of the GC electrode.

To prepare the Pt/MWCNTs paste, 14.4 mg Pt/MWCNTs catalyst was ultrasonic dispersed in a mixture of 5 ml ethanol and 1 ml 0.1% Nafion solution for 30 min. About 10 μl catalyst ink was then spread on the top of the GC electrode and dried at 70 °C, after that 10 μl 0.1% Nafion solution was coated on it as a binder and dried at 70 °C. The metal loading of the electrode was 38 μg cm^{-2}.

The MWCNTs were characterized using cyclic voltammetry (CV) in nitrogen saturated 0.5 M H_2SO_4 within the potential range of –0.241 to 0.8 V. The electrochemical performances of the Pt/MWCNTs catalysts were measured in nitrogen saturated 0.5 M H_2SO_4 with or without 1 M CH_3OH solution at a scan rate of 50 mV s^{-1} at room temperature within the potential range of –0.241 to 1.0 V. All potentials in the paper were referred to SCE.

3 Results and discussion

3.1 Characterization of MWCNTs supports

3.1.1 Physical characterization

Table 1 shows the physical properties of MWCNTs. It can be seen that D10-50 and D10-2 have higher surface areas compared with other samples. The surface area of D3050-2 is 152 m^2 g^{-1}, which is higher than the other CNTs with similar diameters. It is can be seen that the surface areas of MWCNTs decrease with the increase of the tube diameters and lengths. In addition, the conductivities of MWCNTs of fresh and after acids oxidation are summarized in Table 1. It can be found that the conductivities of MWCNTs decrease after acids oxidation compared to fresh MWCNTs. This might be due to the factor of presence of more surface oxides on MWCNTs after acids oxidation. Form Table 1, we can find that D10-2 and D10-50 have higher conductivities than other MWCNTs. XPS was operated to evaluate the oxidation degree of MWCNTs. The atomic ratio O/C values, which are calculated by integrating the area under the high-resolution XPS O 1s and C 1s spectra peaks, are also shown in Table 1. It can be noticed clearly that the ratio of O to C is different for the MWCNTs. The sequence of O/C is: D3050-2 > D10-2 > D10-50 > D4060-15 > D3050-50 > D50-50. D3050-2 has the highest amounts of surface oxidation (O/C = 0.093) and D50-50 has the least (O/C = 0.037).

Figure 1 shows the TEM images of D10-2, D10-50, D3050-2 and D50-50. Compared with other samples, more amorphous carbon and defects are observed on D10-2 and D10-50. This may be interpreted that the sonochemically treatment may cause the roughening of the surface of MWCNTs and the only acid oxidation do not effectively remove the amorphous carbon on the MWCNTs surface [27, 28]. Hou et al. also showed that MWCNTs with smaller diameter contained more amorphous carbon compared to those with larger diameter [29]. In addition, the ends of MWCNTs with large diameter show clear open ends. However, some of the ends of MWCNTs with a diameter of 10 nm seem not to be well opened. By HNO_3 sonochemically treatment, the length and diameter of the MWNCTs are similar to that reported by the manufacturers.

3.1.2 Cyclic voltammetry

Figure 2 shows the CV curves of MWCNTs with different diameters and lengths. A pair of redox peaks appears at 0.34 and 0.28 V, which can be assigned to the redox of surface oxide groups (such as carboxyl, carbonyl and hydroxylic groups) on functional MWCNTs [30]. It can be seen from Fig. 2 that the peak currents increase with the decrease in tube diameter and length. Although the exact number of surface oxide groups cannot be determined, the relative amounts can be roughly estimated from the peak currents [31]. D50-50 has the least peak currents in all the samples, D10-2 and D10-50 have the relatively higher peak currents. It is a little strange that D3050-2 has the highest peak current, which indicates the highest amounts of surface oxide groups. The results agree with the results of XPS. The highest amounts of D3050-2 could be related to the textural properties shown in Table 1 and Fig. 1. The high-surface area and clear open ends could lead to a high concentration of surface oxide groups.

3.2 Characterization of Pt nanoparticles on MWCNTs

3.2.1 TEM analysis of Pt/MWCNTs

The TEM images of Pt nanoparticles supported on various MWCNTs are shown in Fig. 3. The particle sizes determined by TEM are summarized in Table 2. The average particle sizes are about 3.0–3.5 nm for all the samples. It seems that the sizes of the Pt particles are not closely related to the length and diameter of the MWCNTs in this study. However, some isolated Pt clusters aggregate on D10-2 and D10-50, which could lead to a low-Pt utilization. General speaking, larger surface area of the support can result in better Pt

Table 1 Physical properties of different MWCNTs

Tube diameter (nm)	Length (μm)	Surface area (m^2 g^{-1})	Conductivity (S/cm)		O/C (XPS)
			Fresh	After oxidation	
10	~2	452	13.9	10.6	0.061
10	~50	372	12.3	11.6	0.057
30–50	~2	152	12.6	6.92	0.093
30–50	~50	73.6	10.1	9.09	0.045
40–60	~15	71.2	4.11	4.00	0.056
50	~50	71.1	11.1	7.87	0.037

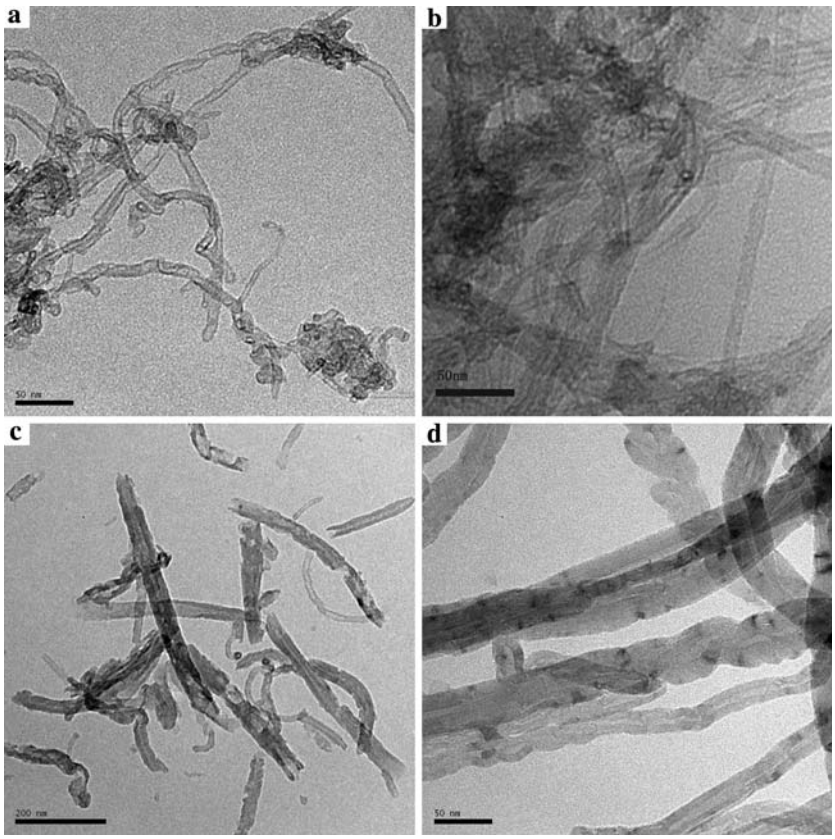

Fig. 1 TEM images of sonochemically-treated MWCNTS (**a**) D10-2, (**b**) D10-50, (**c**) D3050-2 and (**d**) D50-50

dispersion [32]. But in our research, D10-2 and D10-50 have larger surface area and the bad Pt dispersion, which may be attributed to the unclean surface. Furthermore, some Pt particles can be seen in the middle of the tubes for catalysts supported on D3050-2 and D4060-15, as shown in Fig. 3c and d. It is still not clear whether the Pt particles are on inner walls or on outer walls, however, it is expected that some Pt particles can deposit on inner tubes. Because more open ends exist in the MWCNTs with large diameter, which would facilitate the infiltration of H_2PtCl_6 precursor and the deposition of Pt on the inner tubes and at the end of the tips [33]. For the catalysts based on D10-2 and D10-50, almost no Pt particles can be seen in the middle of the tubes.

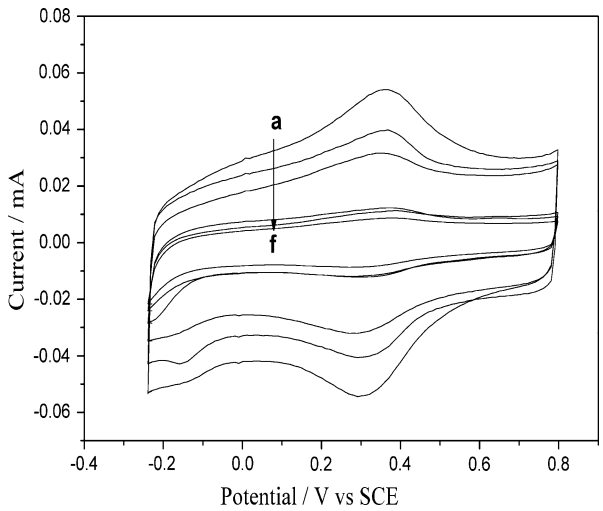

Fig. 2 Cyclic voltammograms of various MWCNTs (a) D3050-2, (b) D10-2 (c) D10-50, (d) D4060-15, (e) D3050-50 and (f) D50-50 (from top to bottom) in 0.5 M H_2SO_4 solution, scan rate 50 mV s^{-1}

The surface oxide groups of the support are usually anchorage sites for the metal precursor during catalyst preparation and can result in good metal dispersion [34, 35]. But there is no agreement about the point. Some studies have showed that the oxidation of active carbon used as support for Pt metal has a negative influence on getting a catalyst with a high dispersion [36, 37]. In our studies, D10-2, D10-50 and D3050-2 have more surface oxides compared to other samples, but D10-2 and D10-50 result in poorer Pt dispersion, D3050-2 results in better Pt dispersion. Connecting the amounts of surface oxide groups (XPS and CV results) and the Pt dispersion, it seems that there is not clear relationship between the both for the samples in the work.

3.2.2 Electrochemical characterization of Pt/MWCNTs

Figure 4 shows CV curves of Pt nanocomposites supported on different MWCNTs in 0.5 M H_2SO_4. Similar

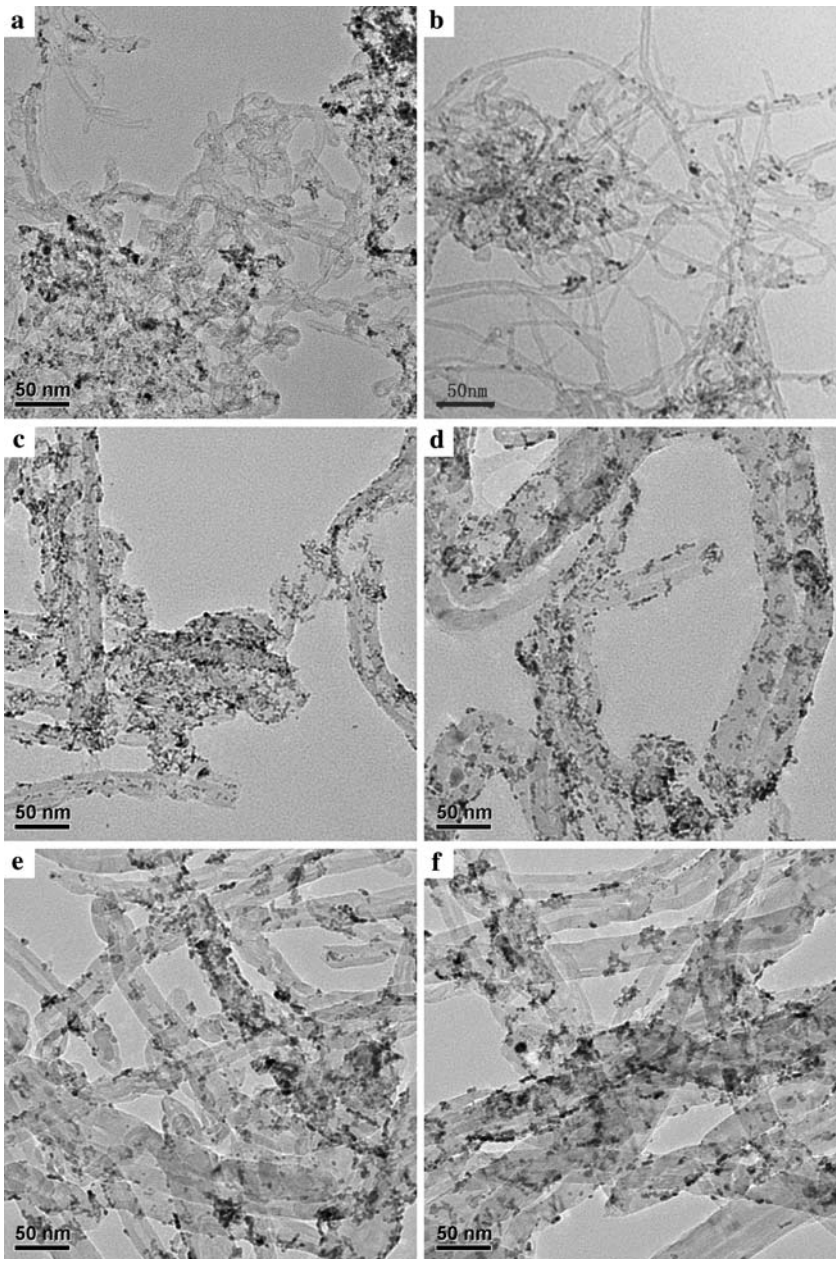

Fig. 3 TEM images of Pt nanocomposites supported on various MWCNTs (**a**) D10-2, (**b**) D10-50, (**c**) D3050-2, (**d**) D 4060-15, (**e**) D3050-50 and (**f**) D50-50

Table 2 Characteristics of Pt/MWCNTs catalysts

Catalyst	Particle sizes (nm)	ECSA ($m^2\ g^{-1}$)	Mass current density (mA mg^{-1})	Specific activity (A m^{-2})
Pt/D10-2	3.0	23.1	241	10.4
Pt/D10-50	3.0	23.2	187	8.1
Pt/D3050-2	2.9	40.5	425	10.5
Pt/D3050-50	3.4	36.5	310	8.5
Pt/D4060-15	3.2	38.5	400	10.4
Pt/D50-50	3.5	32.0	293	9.1

cathodic and anodic peaks in the H-adsorption and H-desorption region (–0.2 to 0.1 V) can be observed for all the samples. The ECSA can be calculated from the charge of hydrogen desorption peak after subtracting the charge from the double-layer region (Q_H) following the next formula, assuming that the smooth Pt electrode

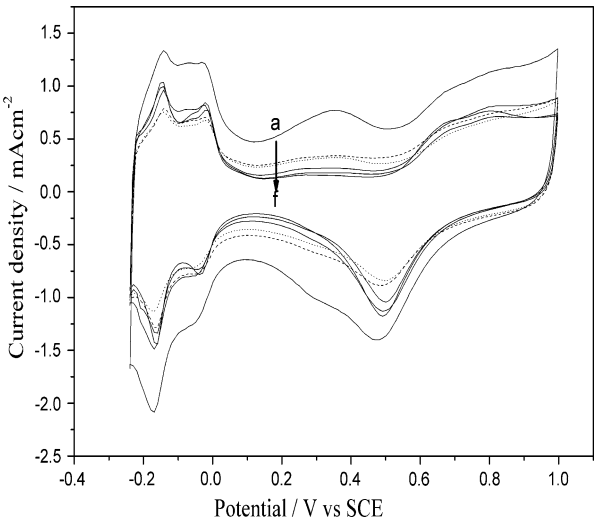

Fig. 4 CV curves of Pt nanoparticles supported on MWCNTs (a) D3050-2, (b) D10-2, (c) D10-50, (d) D4060-15, (e) D3050-50 and (f) D50-50 (from top to bottom) in 0.5 M H_2SO_4 solution, scan rate 50 mV s^{-1}

gives the hydrogen adsorption charge of 0.21 mC cm^{-2} [38].

$$\mathrm{ECSA} = \frac{\mathrm{Q_H}}{0.21 \times m_{\mathrm{Pt}}}, \quad (1)$$

where m_{Pt} represents the Pt loading (g) on the electrode. Q_H (mC) the charge for hydrogen desorption and 0.21 (mC cm^{-2}) is a correspondence value. The calculated ECSAs are listed in Table 2. It can be seen that the Pt catalysts supported on MWNCTs with a diameter about 10 nm show the lowest ECSA among the samples studied. This could be due to the severe aggregation of Pt particles in the catalysts as shown in Fig. 3. The other samples show similar ECSAs. However, the catalysts supported on shorter MWCNTs seem have higher ECSAs than those on longer MWCNTs. This could be related to the large number of edges for short MWCNTs, which could improve the dispersion of Pt particles.

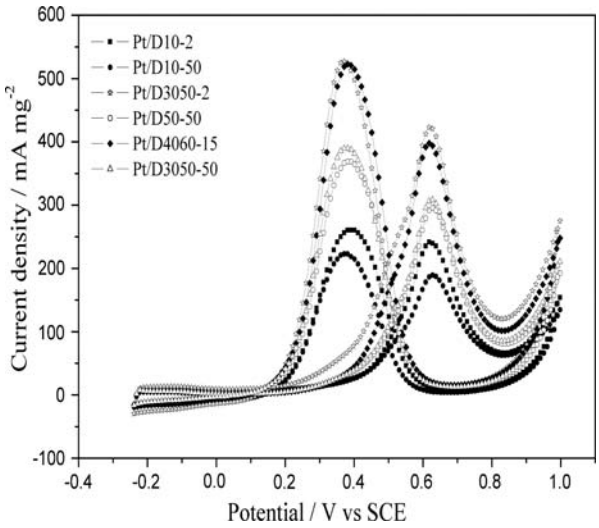

Fig. 5 CV curves of methanol oxidation of Pt/MWCNTs catalysts in 0.5 M H_2SO_4 + 1 M CH_3OH solutions, scan rate 50 mV s^{-1}

Figure 5 shows the electrocatalytic properties towards methanol oxidation of various Pt/MWCNTs catalysts. Typical features of methanol oxidation and subsequent intermediates oxidation at 0.63 and 0.38 V (versus SCE), respectively, are observed. The mass activities of methanol oxidation at peak potential in the forward scan are also summarized in Table 2. The methanol oxidation activities are in the sequence of Pt/D3050-2 > Pt/D4060-15 > Pt/D3050-50 > Pt/D50-50 > Pt/D10-2 > Pt/D10-50. The catalysts supported on MWCNTs with a diameter of 10 nm show much lower activity compared with other catalysts due to the agglomeration of Pt particles, although the conductivities of D10-2 and D10-50 are higher than other MWCNTs. This result suggests that high-Pt dispersion overwhelms the factor of conductivity for methanol electrooxidation in this study. It is essential to have a good Pt dispersion for preparing high-performance electrodes for methanol oxidation with high-Pt utilization.

An obvious effect of the length of MWCNTs on the activities of the catalysts can be observed from Table 2. The catalysts based on short MWCNTs have mass activities 30% higher than those based on long MWCNTs, while the tube diameters are similar. Two reasons could lead to this phenomenon. One is that the short MWCNTs could have better dispersion in the EG solution [39], resulting in better Pt dispersion and utilization. The other reason could be due to the high activity of the ends of MWCNTs. It was reported that the ends of CNTs exhibited higher electrocatalytic properties for epinephrine oxidation compared with the side walls, which could be due to the rapid electron transfer rate [40–42]. Chou et al. [43] also showed that the activity of CNTs increased with the decrease in the length of CNTs.

To further study the effect of tube length, we normalize the mass current densities to ECSAs of Pt as specific activities, which are summarized in Table 2. The ratios of specific activities of Pt/D10-2 to Pt/D10-50, Pt/D3050-2 to Pt/D3050-50 and Pt/D4060-15 to Pt/D50-50 are 1.3, 1.2 and 1.1, respectively. It is obvious that the catalysts supported on short MWCNTs exhibit higher activity due to both the high utilization (dispersion) of Pt and the high-intrinsic activity of the ends of MWCNTs, especially for catalysts supported on MWCNTs with large diameter. It can be concluded that Pt supported on short MWCNTs with suitable diameters would be suitable catalysts with high activity and high-Pt utilization.

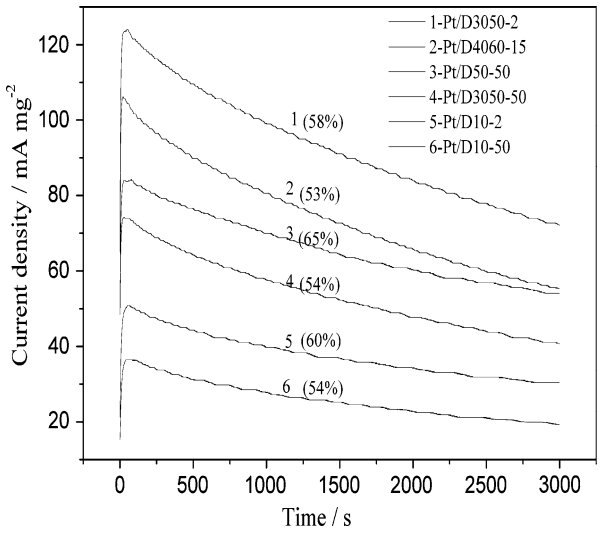

Fig. 6 Chronoamperometry curves of Pt/MWCNTs in 0.5 M H_2SO_4 + 1 M CH_3OH solutions at 0.4 V vs. SCE

Further, we measure the chronoamperometry test of Pt/MWCNTs to study the long-time performance at 0.4 V versus SCE (Fig. 6). It can be seen that the current decreases continuously with time for all the catalysts, which is due to the formation of intermediate poisons like CO_{ad}, CHO_{ad} during the methanol oxidation [44]. The ratios of the current at 3,000 s to the initial current are also shown in Fig. 6. It can be seen that Pt/D50-50 is more tolerant to the poisons. The current is 65% of the initial current after 3,000 s, which is higher than the values of other catalysts. In addition, the current of Pt/D50-50 is higher than Pt/D3050-50 in Fig. 6, although the peak current is a little lower than Pt/D3050-50 (Fig. 5). This may be attributed to the more homogeneous tube diameter distribution of D50-50. At long times, although the current gradually decays for all the catalysts, Pt/D3050-2 maintains the highest current and exhibits the best electrocatalytic activity for methanol oxidation.

4 Conclusion

The amounts of surface oxides of MWCNTs increased with the decrease of the diameters and lengths. But there was no clear relationship between the Pt dispersion and the amounts of surface oxides of MWCNTs in our studies. The morphology of MWCNTs had strong effect on the dispersion and utilization of Pt as well as the catalysts activities based on it. Pt nanocomposites supported on short MWCNTs with suitable diameters exhibited high activity due to the improvement of Pt utilization and the high-intrinsic activity of the ends of MWCNTs. Pt nanoparticles supported on short MWCNTs with a diameter of 30–50 nm showed the best Pt dispersion and highest methanol oxidation activity among the catalysts studied.

Acknowledgments This work was supported by the NSF of China (20673089, 20273053, 20023001 and 29933040), the 973 programming (001CB108906 and the Key Scientific Project of Fujian Province of China (2005HZ01-3). The authors thank Chengdu Timenano Co. Ltd. and Shenzhen Nanotech Port Co. Ltd. for providing the MWCNTs samples.

References

1. Zhang Y, Li J, Shen Y, Wang M, Li J (2004) J Phys Chem B 108:15343
2. Poh WC, Loh KP, Zhang WD, Triparthy S, Ye JS, Sheu FS (2004) Langmuir 20:5484
3. Sun L, Crooks RM (2000) J Am Chem Soc 122:12340
4. Zhang L, Melechko AV, Merkulov VI, Guillorn MA, Simpson ML, Lowndes DH, Doktycz MJ (2002) Appl Phys Lett 81:135
5. Saito Y, Tsujimoto Y, Koshio A, Kokai F (2007) Appl Phys Lett 90:213108
6. Bonard JM, Weiss N, Kind H, Stocki T, Forro L, Kern K, Chatelain A (2001) Adv Mater 13:184
7. Park C, Anderson PE, Chambers A, Tan CD, Hidalgo R, Rodriguez NM (1999) J Phys Chem B 103:10572
8. Fan YY, Liao B, Liu M, Wei YL, Lu MQ, Cheng HM (1999) Carbon 37:1649
9. Zheng JS, Zhang XS, Li P, Zhu J, Zhou XG, Yuan WK (2007) Electrochem Commun 9:895
10. Prabhuram J, Zhao TS, Tang ZK, Chen R, Liang ZX (2006) J Phys Chem B 110:5245
11. Planeix JM, Coustel N, Coq B, Brotons V, Kumbhar PS, Dutartre R, Geneste P, Bernier P, Ajayan PM (1994) J Am Chem Soc 116:7935
12. Mubeen S, Zhang T, Yoo B, Deshusses MA, Myung NV (2007) J Phys Chem C 111:3621
13. Satishkumar BC, Vogl EM, Govindaraj A, Rao CNR (1996) J Phys D: Appl Phys 29:3173
14. Cui HF, Ye JS, Liu X, Zhang WD (2006) Nanotechnology 17:2334
15. Steigerwalt ES, Deluga GA, Lukehart CM (2002) J Phys Chem B 106:760
16. Wu G, Chen YS, Xu BQ (2005) Electrochem Commun 7:1237
17. Kim C, Kim YJ, Kim YA, Yanagisawa T, Park KC, Endo M, Dresselhaus MS (2004) J Appl Phys 96:5903
18. Wang X, Li M, Chen Z, Waje M, Yan Y (2006) J Power Sources 158:154
19. Tang H, Chen JH, Hung ZP, Wang DZ, Ren ZF, Nie LH, Kuang YF, Yao SZ (2004) Carbon 42:191
20. Liu Z, Lin X, Lee JY, Zhang W, Han M, Gan LM (2002) Langmuir 18:4054
21. Britto PJ, Santhanam KSV, Julio AR, Ajayan PM (1999) Adv Mater 11:154
22. Huang JE, Guo DJ, Yao YG, Li HL (2005) J Electroanal Chem 577:93
23. Li WZ, Wang X, Chen ZW, Waje M, Yan YS (2006) J Phys Chem B 110:15353
24. Yuan FL, Ryu HJ (2004) Nanotechnology 15:S596
25. Tang H, Chen JH, Huang ZP, Wang DZ, Ren ZF, Nie LH, Kuang YF, Yao SZ (2004) Carbon 42:191
26. Xing Y (2004) J Phys Chem B 108:19255
27. Hull RV, Li L, Xing YC, Chusuei CC (2006) Chem Mater 18:1780

28. Lordi V, Yao N, Wei J (2001) Chem Mater 13:733
29. Hou PX, Xu ST, Ying Z, Yang QH, Liu C, Cheng HM (2003) Carbon 41:2471
30. Chen JM, Wang MY, Liu B, Fan Z, Cui KZ, Kuang YF (2006) J Phys Chem B T110TT:11775
31. Xing Y, Li L, Chusuei CC, Hull RV (2005) Langmuir 21:4185
32. Takasu Y, Kawaguchi T, Sugimoto W, Murakami Y (2003) Eletrochim Acta 48:3861
33. Yang CW, Hu XG, Wang DL, Dai CS, Zhang L, Jin HB, Agathopoulos S (2006) J Power Sources 160:187
34. Noh JS, Schwartz JA (1990) Carbon 28:675
35. Foger K (1984) Catalysis science and technology, vol 6. Springer, Heidelberg
36. Van Dam HE, Bekkun HV (1991) J Catal 131:335
37. Czaran E, Finster J, Schnabel H, Anorg Z (1978) Allg Chem 443:175
38. Tian ZQ, Jiang SP, Liang YM, Shen PK (2006) J Phys Chem B 110:5343
39. Li ZF, Luo GH, Zhou WP, Wei F, Xiang R, Liu YP (2006) Nanotechnology 17:3692
40. Banks CE, Moore RR, Davies TJ, Compton RG (2004) Chem Commun 16:1804
41. Li J, Cassell A, Delzeit L, Han J, Meyyappan M (2002) J Phys Chem B 106:9299
42. Gooding JJ, Wibowo R, Liu JQ, Yang WR, Losic D, Orbons S, Mearns FJ, Shapter JG, Hibbert DB (2003) J Am Chem Soc 125:9006
43. Chou A, Böcking T, Singh NK, Gooding JJ (2005) Chem Commun 7:842
44. Kabbabi A, Faure R, Durand R, Beden B, Hahn F, Leger JM, Lamy C (1998) J Electroanal Chem 444:41